Science and Technology Indonesia
e-ISSN:2580-4391 p-ISSN:2580-4405
Vol. 11, No. 3, July 2026

Research Paper

Temperature Estimation of Geothermal Systems and Subsurface Model Based on Geochemical of Lake Ranau

Mochammad Malik Ibrahim[1*], Agung Harijoko[2], Wiwit Suryanto[3]

[1]Department Geological Engineering, Sriwijaya University, South Sumatra, 30662, Indonesia
[2]Departement of Geological Engineering, Gadjah Mada University, Yogyakarta, 55281, Indonesia
[3]Departement of Physics, Gadjah Mada University, Yogyakarta, 55281, Indonesia
*Corresponding author: malikibrahim100@ft.unsri.ac.id

Abstract
The geothermal potential in the Lake Ranau area comes from the remnants of the magmatic activity from Mount Seminung. Geothermal manifestations in the research area are indicated by the presence of hot springs dan controlled by geological structures. This research aims to determine estimated geothermal system temperatures and subsurface model based on chemical geothermometer analysis. The chemical geothermometer method is used to indirectly estimate the temperature of subsurface geothermal system. Geothermal fluid manifestations in Kota Batu Village were chemically sampled by collecting three samples (LP 1 – LP 3) and Lombok Village by collecting three samples (LP 4 – LP 6). Chemical geothermometers used in the research are silica, Na/K, K/Mg and Na−K−Ca geothermometers. The results of chemical geothermometer calculations on six samples from geothermal fluid manifestation locations, determination of subsurface reservoir temperature of the geothermal system in research area ranges 177.0 - 285.6°C and included in the geothermal system with intemediate to high enthalpy. The subsurface model based on the calculation results of various chemical geothermometers about geothermal system components such as cap rock, reservoir rock, heat source, geological structure, thermal fluid and surface manifestations.

Keywords
Geothermal Potential of Lake Ranau, Chemical Geothermometer, Temperature Estimation, Subsurface Model

Received: 26 January 2026, Accepted: 18 March 2026
https://doi.org/10.26554/sti.2026.11.3.773-783

1. INTRODUCTION

Indonesia is located on three major tectonic plates (Eurasian, Indo-Australian and Pacific), making it a complex tectonic setting. This position makes Indonesia part of the Pacific Ring of Fire (Hartati et al., 2026). The Pacific volcanic belt in some parts of Indonesia and tectonic setting is considered to be the basis for the formation Kasbani (2009). Geothermal systems in Indonesia are generally high-temperature hydrothermal systems (>225°C) (Saptadji, 2009). Most of the developed geothermal fields in Indonesia are volcano-hosted high-temperature resources, providing abundant lessons learned for developing potential high temperature resources in the future (Shalihin et al., 2024).

Based on data from the (Geological Agency, 2023), geothermal potential in Indonesia reaches 23,765 GW and 361 location points in 30 provinces. According to 2023 data from the Coal and Geothermal Mineral Resources Center, there are 55 potential points, 42% of which are classified as high temperature geothermal resources, 71 potential points, 54% as intermediate temperature geothermal resources and the rest as low temperature geothermal resources. According to the Directorate General of EBTKE (2023), the realized installed capacity of EBT power plants reached 13.155 MWe or 13.16 GW in 2023, including 2.417.7 MWe of geothermal power plants (Ministry of Energy and Mineral Resources, 2024). History of geothermal exploration in Indonesia began in 1970 to discover and develop high temperature geothermal systems. Detailed prospecting exploration discusses geological, geochemical and geophysical methods are combined to assess the field characteristics when defining exploration wells in order to predict the presence of high temperatures (Hochstein and Sudarman, 2008).

Sumatra Island is tectonically controlled by the oblique subduction of the Indo-Australian Plate to the Eurasian Plate. This process triggers the formation of the Great Sumatra Fault (GSF), a series of quaternary volcanic activity and a geothermal system that develops along the tectonic line (Khakim et al., 2023). There are two main types of geothermal systems in Sumatra, the first is located on the slopes of volcanoes and the second is located in pull-apart basins along the Sumatra fault. The latter type formed as thirteen pull-apart basins due to a specific tectonic setting in the main Sumatran strike-slip fault and volcanic zone in Sumatra (Muraoka et al., 2010).

The geothermal potential in the Lake Ranau area comes from the remnants of the magmatic event associated with Mount Seminung. This tectonic setting created the lake and caused fractures in the area. These fractures subsequently served as pathways for magma to reach the Earth's surface. Additionally, indications of the influence of the Liwa Fault located were also found in the research area. This Liwa Fault structure is an active fault within the Sumatra Fault System (Aribowo et al., 2017). The Ranau Lake geothermal area is a geothermal prospect in Indonesia and consist of eight hot springs and two altered rocks. All hot springs are located in edge of the lake (Wioso et al., 2022).

In the research area, there have been studies on quartz geothermometers by Zainal et al. (2024) and isotope geothermometer by Ibrahim et al. (2024b). The calculation results show that the quartz geothermometer gives reservoir temperature estimates of 280.5°C and the isotope geothermometer gives reservoir temperature estimates of 270°C. Another research by Afiat et al. (2020) that numerical model simulation of geothermal reservoir temperature estimates for Lake Ranau of 200–269°C. This result shows that the geothermal potential in the area belongs to the high temperature category. The integrated geothermometer approach enhances confidence in determining reservoir temperature limits and developing conceptual subsurface models. This research applies several chemical geothermometers and statistical analysis integration.

Chemical geothermometers are the most commonly used method for determining reservoir temperature in geothermal systems. This geothermometer consists of equations calibrated empirically or theoretically based on heterogeneous chemical reactions that depend on temperature, which control the concentration of specific solutes in equilibrium conditions (Jiménez et al., 2026). The chemical geothermometer method can be used to predict the temperature of geothermal systems indirectly at a cost is not too expensive, but the results do not deviate far from the actual conditions in nature (subsurface). The principle of geothermometers is based on the chemical behavior of elements dissolved in geothermal fluids. This research expands the interpretation by applying a multicomponent chemical geothermometer framework and integrating equilibrium sensitivity analysis and mixing interpretation. This approach is more comprehensive of reservoir conditions and subsurface system behavior than relying on temperature estimates using a single method.

2. EXPERIMENTAL SECTION

2.1 Location of Research Area

The research area is administratively located at coordinates UTM 380.000 mE – 392.000 mE and 9.462.000 mN – 9.449. 200 mN, covering an area of approximately 127 km^2 (Ibrahim et al., 2022). The Ranau Lake geothermal research area covers

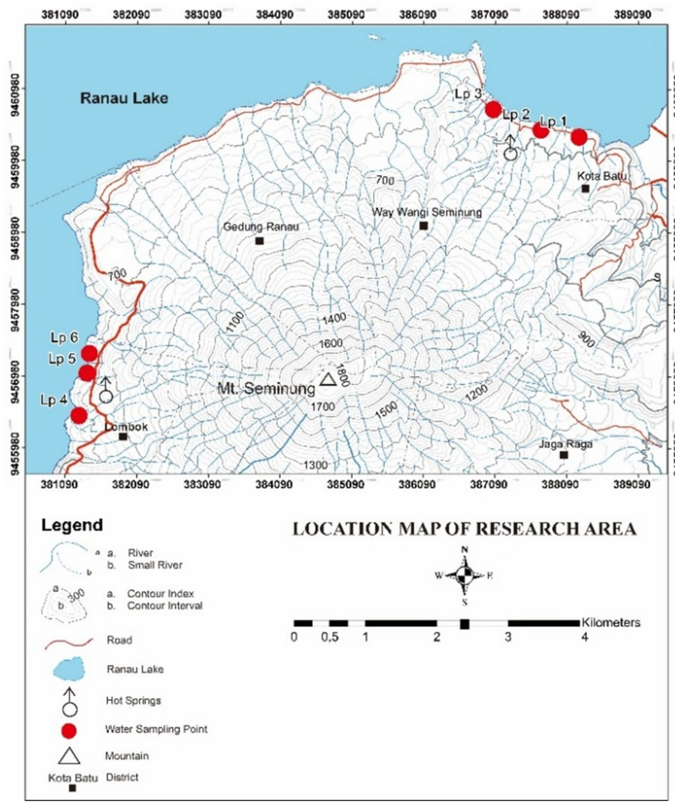

Figure 1. Location Map of Research Area (Modification (Ibrahim et al., 2022))

an area of about 12 × 13 km^2 at an altitude of 500 - 1800 msl as shown in Figure 1. This research aims to calculate the estimated temperature of the geothermal system and subsurface model based on the analysis of chemical geothermometer method. Six samples were collected from two main manifestations (Kota Batu and Lombok), which correspond to the outflow zone. These locations represent the dominant hydrothermal discharge areas identified in the geological investigation. Sampling focused on geochemically active zones and most of these areas show surface manifestations.

The geology of the Ranau Lake area was consists of quaternary deposits and tertiary rock formations. Quaternary deposits consist of alluvial deposits, Kukusan volcano deposits, Seminung volcano deposits and Pugung volcano deposits as shown in Figure 2. The stratigraphy of rock formations from youngest to oldest during the Tertiary period consists of the Ranau Formation, Bal Formation and Hulusimpang Formation (Ibrahim et al., 2020). The emergence of discharge zone on the surface is marked by surface manifestations arising from lithological contacts and faults formed around Mount Seminung, located in the Kota Batu and Lombok regions (Geological Resources Center, 2004).

The Lake Ranau area is known to have two geological structures which contribute to the process of geothermal fluid uplift, namely structures with the direction of N 289° E and N 008°

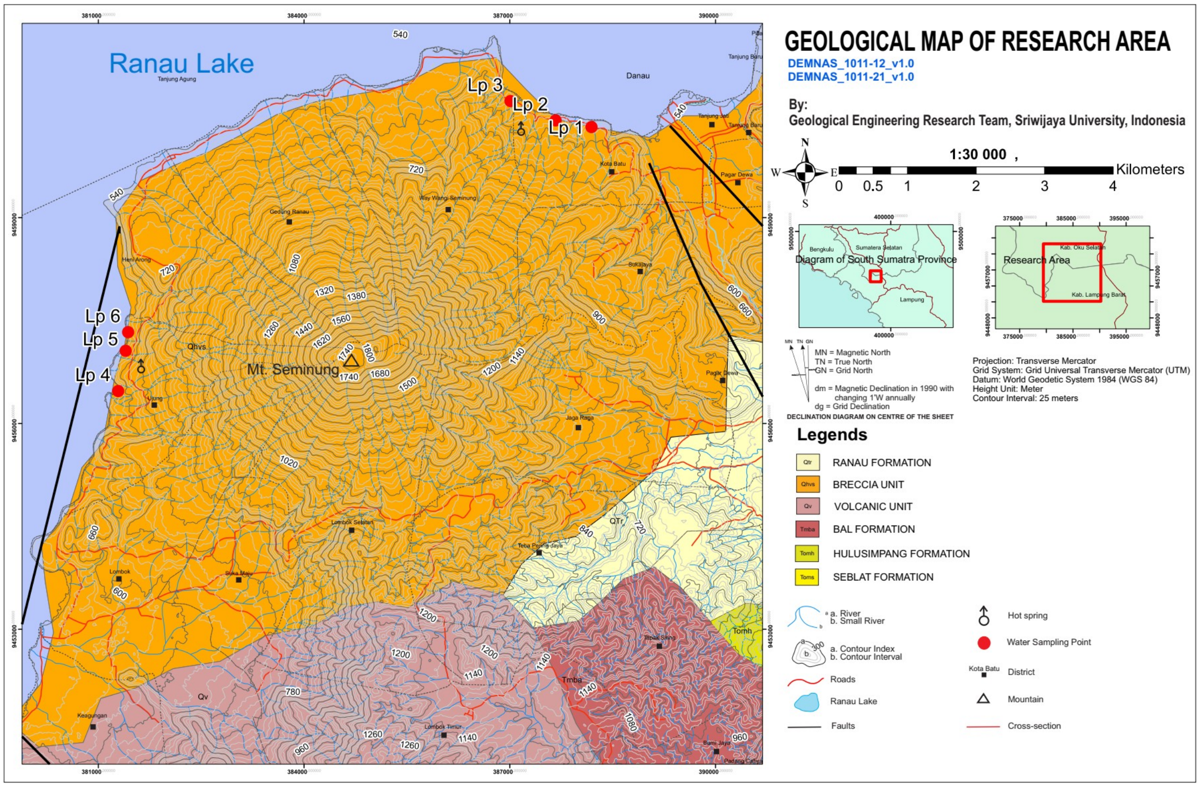

Figure 2. Geological Map of Research Area (Ibrahim et al., 2020)

E (Sugianto and Muttaqin, 2011). In the direction of N 289° E is known as the Kota Batu Fault, which is a normal fault with a main north-south orientation. Meanwhile, the N 008° E fault is the Lombok Fault, which is also a normal fault with a hanging wall position located in the western part of Mount Seminung.

2.2 Materials and Procedure Collect Data

The research method consists of steps taken by researchers to collect data that will be processed and analyzed scientifically. Geothermal fluid manifestations in Kota Batu Village were chemically sampled by collecting three samples (LP 1 – LP 3) and Lombok Village by collecting three samples (LP 4 – LP 6). The research method used Atomic Absorption Spectrometer (AAS), Turbidimetry and Titrimetry to measure anion and cation content parameters in water samples. The anion and cation content is used for the calculation of various types of chemical geothermometers.

2.3 Water Chemical Analysis and Geothermometer

The units of cation and anion concentration data in mg/L were converted to meq/L based on the atomic mass of each ion. To ensure the accuracy of cation and anion ion concentration data, the percentage of Charge Balance Error (CBE) was calculated. CBE calculation is based on the law of conservation of charge, which is a fundamental principle in solution chemistry (Domenico and Schwartz, 1998). If the CBE value is <5% then the charge balance is good (data is acceptable) and if the CBE value is >5% then there may be errors in the analysis or calculation. Calculation of CBE percentage value, as shown in Equation (1) as follows:

$$\text{CBE}(\%) = \left(\frac{\sum \text{cation} - \sum \text{anion}}{\sum \text{cation} + \sum \text{anion}}\right) \times 100 \tag{1}$$

Chemical geothermometers are an important geochemical method for geothermal resource exploration and development. Geothermometers are used to estimate subsurface temperatures (Karingithi, 2009). This method is used based on the development of empirical geothermometers involving a number of chemical elements (Na, K, Ca, Mg, and SiO_2). Chemical elements can be used in calculations using geothermometer formulas. The RMS error value of the temperature calculated using the geothermometer formula has a value of >5% (Utami et al., 2019). There are several types of geothermometers used as parameters to estimate temperature of subsurface geothermal systems are as follows:

1) Calculation of Silica Geothermometer (SiO_2)
   The silica geothermometers is used to measure the solubility of various types of silica in water as a function of temperature. Silica geothermometers generally have temperatures >180°C and exist in quartz equilibrium. The temperature stability of silica reaches 250°C and lowest solubility relative to polymorphic silica. Quartz

geothermometers are most commonly used to measure reservoir temperatures >150°C and <150°C silica content controlled by chalcedony (Fournier, 1977). High silica element can indicate the possibility of geothermal fluid originating from the reservoir. The silica geothermometer is used to calculate subsurface temperature using Equation (2) in the quarz no steam loss and Equation (3) in the quartz max steam loss as follows:

a) Calculation of quartz no steam loss

$$T(°C) = \frac{1309}{5.19 - \log(SiO_2)} - 273.15 \quad (2)$$

b) Calculation of quartz max steam loss

$$T(°C) = \frac{1522}{5.72 - \log(SiO_2)} - 273.15 \quad (3)$$

The quarz no steam loss is used during sampling and not boiling condition, indicating a process of heat release. The quartz max steam loss is used during sampling and boiling condition (± 100°C), indicating no heat release process when the water rise to the surface (Karingithi, 2009).

2) Calculation of Na/K Geothermometer
The Na−K geothermometer is used to chloride water reservoirs with T >180°C. This geothermometer has the advantage of being unaffected by steam loss and dilution (mixing). However, this geothermometer is less accurate when used at T <100°C (Simmons, 1988). The use of this geothermometer considers the relationship between sodium feldspar (Na) and potassium feldspar (K). Na−K geothermometers are used to calculate subsurface temperatures with calculation formulas by several experts in Equations (4), (5) and (6) as follows:

a) Calculation of Na−K geothermometer by Truesdell (1976)

$$T(°C) = \frac{856}{0.857 + \log\left(\frac{Na}{K}\right)} - 273.15 \quad (4)$$

b) Calculation of Na−K geothermometer by Fournier (1979)

$$T(°C) = \frac{1217}{1.438 + \log\left(\frac{Na}{K}\right)} - 273.15 \quad (5)$$

c) Calculation of Na−K geothermometer by Giggenbach (1988)

$$T(°C) = \frac{1390}{1.75 + \log\left(\frac{Na}{K}\right)} - 273.15 \quad (6)$$

3) Calculation of K/Mg Geothermometer
The K/Mg geothermometer is used to calculate the ratio between K and Mg content, where shallow water has a higher Mg content than deeper water. The K/Mg ratio indicates the end condition of the reaction between fluid and rock at the surface. The K/Mg geothermometer is used to calculate subsurface temperature in Equation (7) according to Giggenbach (1988) as follows:

$$T(°C) = \frac{4410}{13.95 + \log\left(\frac{K^2}{Mg}\right)} - 273.15 \quad (7)$$

This geothermometer is commonly used at temperatures of 100 - 300°C with Mg concentrations <0.01 mg/L and most widely used in the research of low to intermediate systems when equilibrium is reached between fluid and mineralogy composition (muscovite-clinoclore-k-feldspar) of the host rock (Giggenbach, 1988).The water maturity can be assessed from the contents of Na, K, and Mg by plotting the values on a Na−K−Mg diagram (Giggenbach, 1988). The presence of Mg is element with low concentration at high temperatures (0.01–0.1 ppm), caused by dilution (mixing) surface water containing high concentrations of Mg (Ellis and Mahon, 1977).

4) Calculation of Na−K−Ca Geothermometer
The Na−K−Ca geothermometer is a type of geothermometer proposed by Fournier and Truesdell (1973) and used in geothermal fluids with high calcium (Ca) concentrations. The K/Mg geothermometer is used to calculate subsurface temperature in Equation (8) according to Fournier and Truesdell (1973) as follows:

$$T(°C) = \frac{1647}{\log\left(\frac{Na}{K}\right) + \beta\left[\log\left(\frac{\sqrt{Ca}}{Na}\right) + 2.06\right] + 2.47} - 273.15 \quad (8)$$

Application terms of Na−K−Ca geothermometer, as follows:

a) If the value of $\left[\log\left(\frac{\sqrt{Ca}}{Na}\right) + 2.06\right] < 0$, then $\beta = \frac{1}{3}$ and T is calculated in $°C$.
b) If the value of $\left[\log\left(\frac{\sqrt{Ca}}{Na}\right) + 2.06\right] > 0$, then $\beta = \frac{4}{3}$ and the calculated $T < 100°C$ is acceptable. If the calculated $T > 100°C$, then recalculate T with $\beta = \frac{1}{3}$.

This geothermometer provides good results for use in high temperature reservoirs (>180°C), but poorly when used at low temperatures. This is caused by the geothermometer being affected by partial pressure of carbon dioxide in solution, interrupted exchange reactions with other ions (especially Mg) and precipitation of calcite with the loss of carbon dioxide from solution during boiling (Nicholson, 1993).

5) Integration of Multiple Geothermometers

The integration of multiple geothermometer approach is expected to enable more reliable assessment of target reservoir temperatures, which could potentially reduce geothermal exploration and development costs (Spycher et al., 2014). Each geothermometer is assessed according to the principles of equilibrium and sensitivity to processes of steam loss, dilution (mixing) and Mg addition. Statistical consistency (mean, standard deviation and coefficient of variation) is evaluated for each geothermometer to ensure internal consistency prior to interpretation. The final reservoir temperature is determined through an integration approach based on the mean calculation of all geothermometer results.

6) Classification of Geothermal Systems Based on Reservoir Enthalpy
The classification of geothermal systems based on reservoir enthalpy according to (Hochstein, 1990), is divided into three categories (Table 1) as follows:

Table 1. Reservoir Enthalpy Classification (Hochstein, 1990)

Classification	Reservoir Enthalpy (°C)
Low Enthalpy	< 125
Intermediate Enthalpy	125 – 225
High Enthalpy	> 225

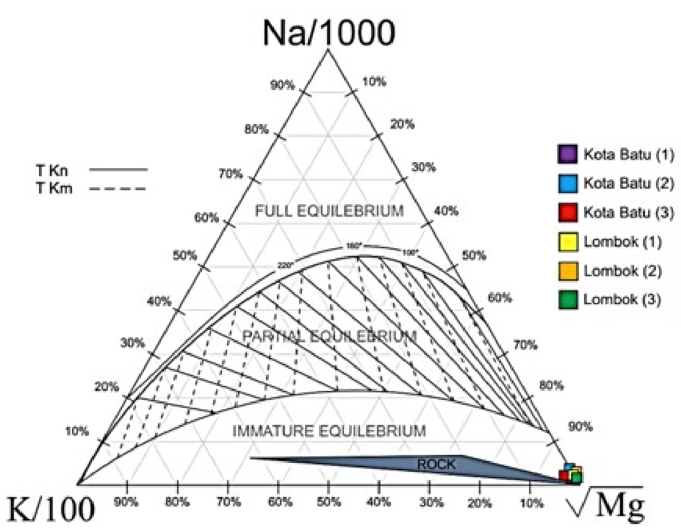

Figure 3. Giggenbach Na−K−Mg Diagram

3. RESULTS AND DISCUSSION

This research uses Atomic Absorption Spectrometer (AAS), Turbidimetry, and Titrimetry analysis in the laboratory to measure the parameters of cation and anion ion content in water samples. Atomic Absorption Spectrometry (AAS) uses multi-point standard solutions with a correlation coefficient >0.995 (Salih, 2024). Analytical accuracy is better than ± 3% based on repeat measurements and the detection limit for major cations (Na, K, Ca, Mg) is within the ppm range according to instrument specifications. Turbidimetry (for SO_4^{2-} analysis) has an accuracy within ±5%, with a detection limit in accordance with standard laboratory procedures (Kelley et al., 2014). Titrimetry (for Cl^- and alkalinity) has an analytical uncertainty within ± 2–5%, depending on the concentration range, based on repeated titration tests and verification of standard solutions (American Public Health Association, 2017).

3.1 Water Samples Concentration

The results of laboratory analysis for the chemical characteristics of water in the research area resulted in the values of cation and anion ions contained in the water (Table 2) as follows:

3.2 Silica Geothermometer

(SiO_2) The results of silica geothermometer (SiO_2) calculations according to Fournier (1977) show that the temperature no steam loss ranges 177.0 to 184.0°C and the maximum steam loss ranges 165.7 to 171.5°C (Table 3). The lowest temperature value was found in Kota Batu (3). The highest temperature value was found in Lombok (3). Silica geothermometer calculations reached a temperature of T >150°C, so that the silica content was not controlled by chalcedony.

3.3 Na-K Geothermometer

The results of Na-K geothermometer calculations according to three reference sources (Table 4). Na-K geothermometer calculations based on Truesdell (1976) produced temperature values ranges 220.7 to 263.6°C. Calculations of the Na-K geothermometer according to Fournier (1979) produced temperature values ranges 165.7 to 171.5°C. Calculations of the Na-K geothermometer according to Giggenbach (1988) produced temperature values ranging from 256.2 to 285.6°C.

Based on the lowest temperature recorded in Lombok (3) and the highest temperature recorded in Kota Batu (3). The Na-K geothermometer calculation shows a temperature of T >180°C, independent of dilution (mixing) or steam loss.

3.4 K/Mg Geothermometer

The results of K/Mg geothermometer calculation according to Giggenbach (1988) produced temperature values ranges 70.9 to 86.3°C (Table 5). The lowest temperature value was found in Kota Batu (1) and the highest temperature value was found in Lombok (1). The K/Mg geothermometer calculation reached a temperature of T <100°C with a Mg contens >0.01 mg/L and influenced by the equilibrium between fluid composition and mineralogy (muscovite-clinoclore-k-feldspar) of the host rock. Therefore, the K/Mg geothermometer calculation results are not used in reservoir temperature conditions.

Temperature estimations using the K/Mg geothermometer are comparatively low, which is inconsistent with the intermediate to high enthalpy classification. The K/Mg geothermometer is strong sensitivity to magnesium enrichment, which frequently happens as a result of interaction with shallow groundwater or poor chemical equilibrium during fluid ascent. The

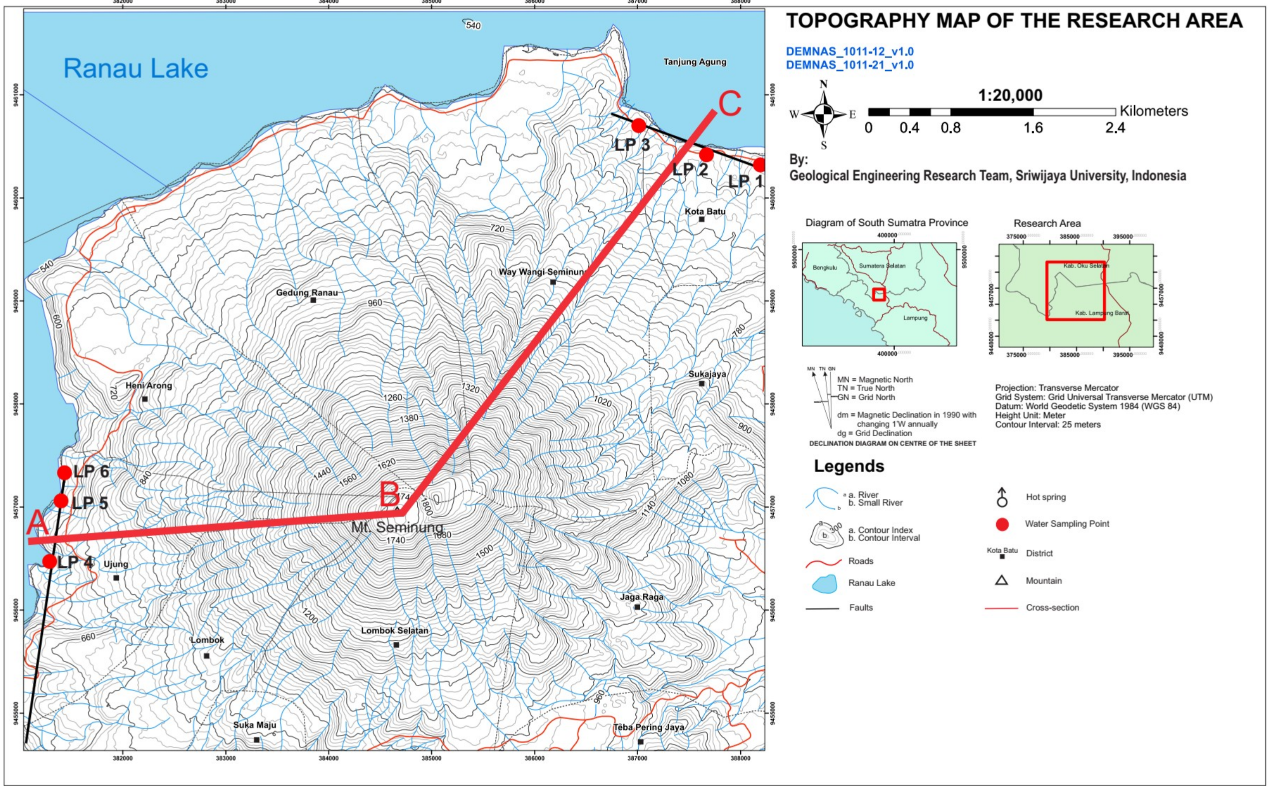

Figure 4. Topographic Map With A-B-C Cross Section

Table 2. Water Samples Concentration of Major Ion Content

Location	Ion Content Parameters							CBE (%)
	Cations (meq/L)				Anions (meq/L)			
	Na	K	Ca	Mg	Cl	HCO_3	SO_4	
Kota Batu (1)	4.49	0.47	3.46	1.86	3.76	4.82	1.35	1.73
Kota Batu (2)	4.60	0.47	3.30	1.73	3.20	5.01	1.15	3.80
Kota Batu (3)	4.52	0.49	3.53	1.76	3.20	5.10	1.15	4.30
Lombok (1)	11.61	0.98	4.24	2.27	4.33	7.75	5.80	3.30
Lombok (2)	11.02	0.97	4.49	3.08	4.33	7.98	6.26	2.60
Lombok (3)	10.69	0.83	4.31	3.05	4.33	7.47	5.66	3.91

higher water rises to the surface and the higher concentration magnesium dissolved (Ibrahim et al., 2024a).

The Giggenbach (1988) Na−K−Mg diagram shows that Mg content is very dominant relative to Na and K content and classifies all samples as immature water, as shown in Figure 3. Water classified in the immature water shows the dominant influence of surface water or meteoric water. The high Mg content in water indicates rock dissolution (leaching) near the surface. The immature water condition is also caused by high temperature and pressure prior to reaching the surface.

3.5 Na−K−Ca Geothermometer

The results of Na−K−Ca geothermometer calculations according to Fournier and Truesdell (1973) produced temperature values ranges 189.7 to 197.0°C (Table 6). The lowest temperature value was found in Lombok (3) and the highest temperature value was found in Lombok (2). Na−K−Ca geothermometer calculations indicate a temperature T >180°C, which was not affected by CO_2 partial pressure, exchange reactions (especially Mg) and precipitation from the solution during the boiling process.

3.6 Temperature Estimation of Geothermal Systems

The results of the calculation differences for subsurface temperatures using chemical geothermometers (Table 7). This is very likely to occur because when geothermal fluids from beneath the surface of the geothermal system move toward the surface, the fluids become contaminated by other chemical elements,

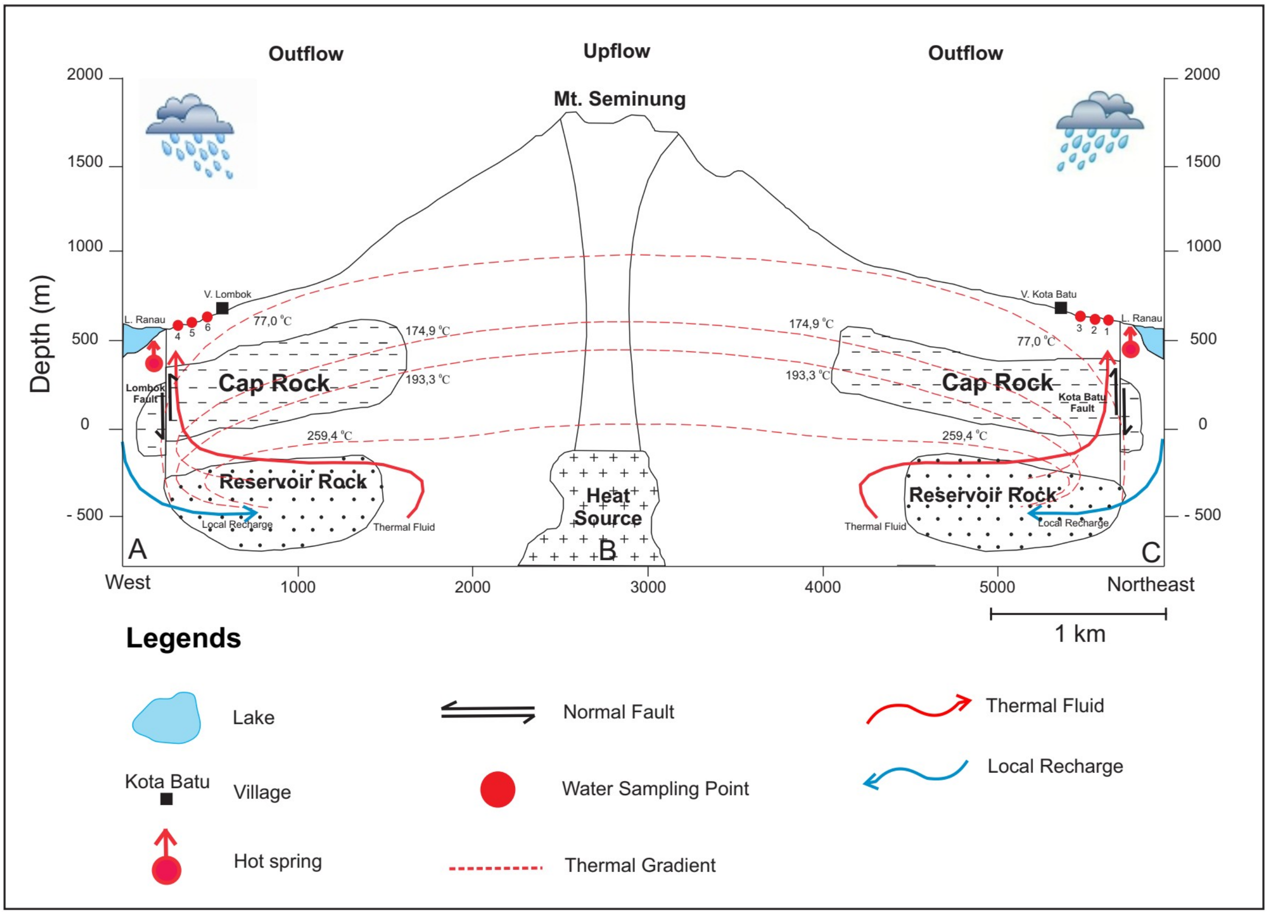

Figure 5. Subsurface Geothermal System Model in Research Area

Table 3. Silica Geothermometer (SiO_2)

Location	SiO_2 (mg/L)	No Steam Loss (°C)	Max Steam Loss (°C)
Kota Batu (1)	204.68	181.5	169.4
Kota Batu (2)	194.2	178.0	166.5
Kota Batu (3)	190.91	176.8	165.6
Lombok (1)	204.37	181.4	169.3
Lombok (2)	211.42	183.8	171.2
Lombok (3)	211.75	183.9	171.3

rocks, dissolution and dilution (mixing) with shallow fluids, thereby forming a new equilibrium.

Based on all geothermometer results, the reservoir conditions in the research area were classified as intermediate to high enthalpy according to Hochstein (1990). The high enthalpy classification is determined by Na–K geothermometer, which consistently temperatures exceed 225°C. The intermediate enthalpy classification is determined by silica and Na–K–Ca geothermometers, which consistently temperatures 125-225 °C. The K-Mg geothermometer has a temperature below 125°C and does not represent reservoir conditions.

The overall range (171–285°C) appears wide when the extreme values of various geothermometers are compared, but each type of geothermometer shows low standard deviation and low coefficient of variation. A coefficient of variation (CV) value <10% indicates that the data variation is relatively low and the estimated results can be considered relatively consistent and stable. This indicates that the wide range does not reflect statistical dispersion, but rather systematic differences between geothermometer principles (silica equilibrium vs. alkali feldspar equilibrium vs. Mg reaction).

Na–K and Na–K–Ca geothermometers are less sensitive to steam loss and shallow mixing reflecting reservoir conditions. Silica geothermometers provide an independent equilibrium limit. K/Mg geothermometers are considered indicators of re-equilibrium and shallow fluid interaction rather than primary reservoir temperature due to their high sensitivity to Mg.

The reservoir temperature indicates the presence of a geothe

Table 4. Calculation Results of Na−K Geothermometer

Location	Na (ppm)	K (ppm)	By Truesdell (1976)	By Fournier (1979)	By Giggenbach (1988)
Kota Batu (1)	103.13	18.44	260.5	272.6	283.5
Kota Batu (2)	105.80	18.40	256.5	269.7	280.9
Kota Batu (3)	103.81	18.97	263.6	274.9	285.6
Lombok (1)	266.88	38.23	230.3	250.0	262.9
Lombok (2)	253.39	38.05	236.4	254.7	267.1
Lombok (3)	245.73	32.63	220.7	242.7	256.2

Table 5. Calculation Results of K/Mg Geothermometer

Location	K (ppm)	Mg (ppm)	K/Mg Geothermometer (°C)
Kota Batu (1)	18.44	22.60	70.9
Kota Batu (2)	18.40	21.04	71.7
Kota Batu (3)	18.97	21.39	72.2
Lombok (1)	38.23	27.54	86.3
Lombok (2)	38.05	37.37	82.3
Lombok (3)	32.63	37.11	78.6

Table 6. Calculation Results of Na−K−Ca Geothermometer

Location	Na (ppm)	K (ppm)	Ca (ppm)	Na−K−Ca Geothermometer (°C)
Kota Batu (1)	103.13	18.44	69.30	192.3
Kota Batu (2)	105.80	18.40	66.16	191.6
Kota Batu (3)	103.81	18.97	70.75	193.4
Lombok (1)	266.88	38.23	84.87	195.8
Lombok (2)	253.39	38.05	89.95	197.0
Lombok (3)	245.73	32.63	86.31	189.7

rmal system with intermediate to high enthalpy based on the consistent high temperature readings produced by Na–K and Na–K–Ca geothermometers. Chemical geothermometer data collection is the primary basis for the interpretation of reservoir temperatures and the development of conceptual models of subsurface geothermal systems. This emphasizes how crucial it is to use supplementary geophysical or isotopic data in order to increase data accuracy.

A comparison between the current geothermometer measurements and previously published temperature estimates (Tabel 8). Geothermometer results generally indicate that the research area is dominated by intermediate to high reservoir temperatures. The estimated reservoir temperature results are used as the basis for developing subsurface geothermal system model in the research area.

3.7 Subsurface Geothermal System Model

Subsurface geothermal system model based on the chemical geothermometer calculation in the research area can be visualized using cross-sections A-B-C as shown in Figure 4. This cross-section provides an overview of the subsurface geological conditions, including geological structures (faults) and components of the geothermal system.

Subsurface geothermal system model based on the results of various chemical geothermometer calculations as shown in Figure 5. The heat gradient line is derived from the average estimated geothermal system temperature from the K−Mg geothermometer of 77.0°C, silica (SiO_2) geothermometer of 174.9°C, Na−K geothermometer of 259.4°C and Na−K−Ca geothermometer of 193.3°C. This research uses a thermal gradient calculation ranges 30–40°C/km. The reservoir temperature of around 171–285°C indicates an estimated reservoir depth of around 4–7 km, taking into account the uncertainty caused by possible convective heat transfer. Structural geometry parameters indicate the presence of normal faults with directions N 289°E and N 008°E, which are interpreted as permeable upflow conduits, localized convective heat transfer is likely to reduce the effective depth of high temperature fluid circulation relative to conductive estimates. This model also contains information about geothermal system components such as cap rock, reservoir rock, heat source, geological structure, thermal fluid and surface manifestations.

In geothermal systems, hydrological processes occur that involve the movement, distribution and interaction between hot and cold fluids. This movement is influenced by fluid pressure, heat gradient and geological structure. Geological structures (normal faults) play an important role as permeable zones that become pathways for hot fluids to escape to the surface in the hot springs form. The point of geothermal manifestation at the surface is within the outflow zone.

Each geothermometer is evaluated based on steam loss, dilution (mixing) and Mg accumulation processes. The K/Mg geothermometer represent sensitivity to shallow groundwater interaction, indicating re-equilibrium during fluid ascent. Na–K and Na–K–Ca geothermometers represent equilibrium conditions controlled by feldspar minerals in high temperatures and relative resistant to dilution (mixing) effects. Silica geothermometers represent an independent equilibrium limit.

The subsurface geothermal model described in this work is

Table 7. Compilation of Chemical Geothermometer Calculation Data

Location	Types of Geothermometers						
	Silica (SiO_2)		Na-K (°C)			K/Mg (°C)	Na−K−Ca (°C)
	No Steam Loss	Max Steam Loss	(Truesdell, 1976)	(Fournier, 1979)	(Giggenbach, 1988)	(Giggenbach, 1988)	(Fournier and Truesdell, 1973)
Kota Batu (1)	181.5	169.4	260.5	272.6	283.5	70.9	192.3
Kota Batu (2)	178.0	166.5	256.5	269.7	280.9	71.7	191.6
Kota Batu (3)	176.8	165.6	263.6	274.9	285.6	72.2	193.4
Lombok (1)	181.4	169.3	230.3	250.0	262.9	86.3	195.8
Lombok (2)	183.8	171.2	236.4	254.7	267.1	82.3	197.0
Lombok (3)	183.9	171.3	220.7	242.7	256.2	78.6	189.7
Mean	174.9		259.4			77.0	193.3
Reservoir Enthalpy Classification	Intermediate		High			Low (Not Reservoir Conditions)	Intermediate
Standard Deviation	6.77		19.17			6.55	2.7
Coefficient of Variation (%)	3.9		7.4			8.5	1.4

Table 8. Comparison of Reservoir Temperature Estimates and Enthalpy Classification from Geothermometers and Previous Studies

Method	Temperature Estimate (°C)	Reservoir Enthalpy Classification
Silica Geothermometer	174.9	Intermediate
Na−K Geothermometer	259.4	High
K/Mg Geothermometer	77.0	Low (Not Reservoir Conditions)
Na−K−Ca Geothermometer	193.3	Intermediate
Quartz Geothermometer by Zainal et al. (2024)	280.5	High
Isotope Geothermometer by Ibrahim et al. (2024b)	270	High
Numerical Model Simulation by Afiat et al. (2020)	200–269	Intermediate–High

conceptual in nature and mostly derives on chemical geothermometer interpretations and surface geological observations. Uncertainties emerge from assumptions relating to fluid–rock equilibrium, potential mixing with shallow groundwater and variances in geothermometer sensitivity. Alternative interpretations of the subsurface configuration, including differences in reservoir depth, fluid pathways and heat source geometry remain possible.

4. CONCLUSIONS

Based on the results of chemical geothermometer calculations on six samples of geothermal fluid manifestation locations, the estimated temperature of the subsurface geothermal system in the research area ranges 171.2 - 285.6°C. The silica (SiO_2) geothermometer produces temperature estimates ranges 165.6 - 184°C. The Na−K−Ca geothermometer produces estimated temperatures ranges 189.7 - 197.0°C. The K/Mg geothermometer produced temperature estimates ranges 70.9 - 86.3°C. The high Mg concentrations and low K/Mg derived temperatures (<100°C) indicate that geothermal fluids and reservoir minerals are not in equilibrium. The Na–K and Na–K–Ca temperature values are consistently high (>180°C) suggest that deeper reservoir signatures. The geothermal system shows the potential for geothermal resources with intermediate to high enthalpy. The chemical equilibrium relationship between geothermal fluids and reservoir minerals is approximated by chemical geothermometers, this assumption fluid steam loss, dilution (mixing) or re-equilibrium throughout the ascent process. Additional sampling data (temporal and spatial) are not available, this research was conducted on six representative geothermal fluid samples from the main manifestation areas (Kota Batu and Lombok). The subsurface model contains information about geothermal system components such as cap rock, reservoir rock, heat source, geological structure, thermal fluid and surface manifestations. Hydrological processes involving the movement, distribution and interaction between hot and cold fluids. Geological structures (normal faults) play an important role as permeable zones that become pathways for the release of hot fluids to the surface in the hot springs form (outflow zone).

5. ACKNOWLEDGMENT

The authors are grateful to Kota Batu and Lombok Village, as well as the geology students at Sriwijaya University who participated in this research. We would also like to thank the reviewers and editorial team at Science and Technology Indonesia for their valuable input and suggestions, which have helped improve the quality of this manuscript.

REFERENCES

Afiat, O. Idianto, G. F. Rera, G. K. Wardoyo, Sutopo, H. B. Pratama, and M. R. Hamdani (2020). Updated Conceptual Model and Resource Assessment Using Numerical Reservoir Simulation of Danau Ranau Geothermal Field, Indonesia. *IOP Conference Series: Earth and Environmental Science*, **732**; 012027

American Public Health Association (2017). *Standard Methods for the Examination of Water and Wastewater*. American Public Health Association, Washington, DC, 23 edition

Aribowo, S., D. Muslim, D. Winantris, M. R. Natawidjaja, and Daryono (2017). Sub-Segmentation of Faults in the Kumering Segment Between Lake Ranau and Suoh Valley, West Lampung. *Journal of Environment and Geological Disasters*, **8**(1); 31–45

Domenico, P. A. and F. W. Schwartz (1998). *Physical and Chemical Hydrogeology*. John Wiley & Sons, New York, 2 edition

Ellis, A. and W. Mahon (1977). *Chemistry and Geothermal System*. Academic Press, New York

Fournier, R. O. (1977). Chemical Geothermometers and Mixing Models for Geothermal Systems. *Geothermics*, **5**; 41–50

Fournier, R. O. (1979). A Revised Equation for the Na/K Geothermometer. *Geothermal Resources Council Transactions*, **3**; 221–224

Fournier, R. O. and A. H. Truesdell (1973). An Empirical Na-K-Ca Geothermometer of Natural Water. *Geochimica et Cosmochimica Acta*, **37**; 1255–1275

Geological Agency (2023). *Balance Sheet of Mineral, Coal, and Geothermal Resources and Reserves Indonesia's 2023*. Ministry of Energy and Mineral Resources, Indonesia

Geological Resources Center (2004). Integrated Geology, Geochemistry and Geophysics Report for the Lake Ranau Geothermal Area, West Lampung Regency, South Lampung–OKU Selatan, South Sumatra. Technical report

Giggenbach, W. F. (1988). Geothermal Solute Equilibria: Derivation of Na-K-Mg-Ca Indicators. *Geochimica et Cosmochimica Acta*, **52**(12); 2749–2765

Hartati, A. R. Effendie, N. Susyanto, and W. Suryanto (2026). Probabilistic Earthquake Hazard Assessment in Indonesia Using Poisson Model and Spatial Grid Analysis. *Science and Technology Indonesia*, **11**(1); 207–216

Hochstein, M. P. (1990). Classification and Assessment of Geothermal Resources. In *Small Geothermal Resources: A Guide to Development and Utilization*. UNITAR/UNDP Centre on Small Energy Sources, Rome

Hochstein, M. P. and S. Sudarman (2008). History of Geothermal Exploration in Indonesia. *Geothermics*, **37**(3); 253–257

Ibrahim, M. M., H. Halik, S. N. Jati, and P. A. A. Zainal (2024a). Geochemical Analysis Based Geoindicator for Geothermal Fluid Manifestation in The Ranau Lake Area, South Ogan Komering Ulu (OKU), South Sumatra. In *International Conference of Geoscience and Remote Sensing Technology*. Springer, pages 21–33

Ibrahim, M. M., J. Harnani, S. N. Jati, and R. K. Abiyyu (2024b). Origin of Geothermal Fluids and Reservoir Temperature Estimation Using Isotope Analysis in the Ranau Lake Area, South Ogan Komering Ulu (OKU), South Sumatra. *Geological Resources Bulletin*, **19**(3); 161–171

Ibrahim, M. M., R. Pranata, B. S. Nababan, N. Heriani, A. Maharani, A. S. J. Situmorang, D. Puspita, K. P. Landia, and M. S. Harfiandri (2022). Characteristics of Manifestations and Recommendations for Utilizing Geothermal Potential in the Ranau Lake Area, South Ogan Komering Ulu (OKU), South Sumatra Province. In *Proceedings of the AVoER XIV National Seminar*. pages 87–91

Ibrahim, M. M., M. Puspita, D. Andarini, A. G. Marbun, and D. I. Arifianto (2020). Geological Identification and Interpretation Based on Remote Sensing Images of the Ranau Lake Geothermal Area, South Ogan Komering Ulu (OKU), South Sumatra. In *Proceedings of the 2nd National Seminar on Earth Environmental Engineering*, volume 2. pages 21–33

Jiménez, J., M. Á. Marazuela, L. F. Auqué, C. Baquedano, J. Martínez-León, S. Gasco-Cavero, J. C. Santamarta, and A. García-Gil (2026). Multicomponent Solute Geothermometry Coupled with Geochemical Modeling of Secondary Processes in Thermal Waters from Volcanic Islands as a Versatile Tool for Geothermal Exploration: Insights from La Palma (Canary Islands). *Geothermics*, **136**; 103583

Karingithi, C. W. (2009). Chemical Geothermometers for Geothermal Exploration. Short Course IV on Exploration for Geothermal Resources, UNU-GTP, GDC and KenGen

Kasbani (2009). Types of Geothermal Systems in Indonesia and Estimation of Their Energy Potential. *Geological Resources Bulletin*, **4**(3); 23–30

Kelley, C. D., A. Krolick, L. Brunner, A. Burklund, D. Kahn, W. P. Ball, and M. Weber-Shirk (2014). An Affordable Open-Source Turbidimeter. *Sensors*, **14**(4); 7142–7155

Khakim, M. Y. N., T. Tsuji, Erni, A. A. Bama, F. Virgo, M. Irfan, A. K. Affandi, and T. Matsuoka (2023). Monitoring the Muara Laboh Geothermal Field in Indonesia Using the ISBAS Method with Sentinel-1 SAR Images. *Science and Technology Indonesia*, **8**(4); 626–631

Ministry of Energy and Mineral Resources (2024). Performance of the EBTKE Sub-Sector in 2023 and Programs for 2024: Diversification of Biofuel Products and Increased Capacity of Renewable Energy Power Plants. Technical report. Press Release No. 62.Pers/04/SJI/2024

Muraoka, H., M. Takashi, H. Sundhoro, S. Dwipa, Y. Soeda, M. Momita, and K. Shimada (2010). Geothermal Systems Constrained by the Sumatra Fault and Its Pull-Apart Basins in Sumatra, Western Indonesia. In *Proceedings World Geothermal Congress*. Bali, Indonesia, pages 1–9

Nicholson, K. (1993). *Geothermal Fluids: Chemistry and Exploration Techniques*. Springer-Verlag, Berlin

Salih, Q. M. (2024). Developing an Analytical Method Using Atomic Absorption Spectroscopy to Estimate Some Heavy Metals in Medicines, Nutritional Supplements, and Blood. *International Journal of Advanced Chemistry Research*, **6**(1); 95–101

Saptadji, N. M. (2009). Geothermal Reservoir Characteristics. Training Advanced Geothermal Reservoir Engineering. 6-17

Shalihin, M. G. J., T. Larasati, D. Gentana, D. Adityatama, F. R. Fadhillah, A. I. Mustika, V. R. Chandra, G. B. Permadi, and S. A. Pongtuluran (2024). Overview of Future Geothermal Development Plan in Indonesia. In *Proceedings of the 10th Indonesia International Geothermal Convention and Exhibition (IIGCE)*

Simmons, S. F. (1988). Geochemistry Lecture Note. Geothermal Institute, University of Auckland

Spycher, N., L. Peiffer, E. L. Sonnenthal, G. Saldi, M. H. Reed, and B. M. Kennedy (2014). Integrated Multicomponent Solute Geothermometry. *Geothermics*, **51**; 113–123

Sugianto, A. and Y. A. Muttaqin (2011). Magnetotelluric Survey of the Way Selabung Geothermal Area, South Oku Regency, South Sumatra. Technical report

Truesdell, A. H. (1976). Summary of Section III: Geochemical Techniques in Exploration. In *Proceedings of the 2nd U.N. Symposium on the Development and Use of Geothermal Resources*. U.S. Government Printing Office, Washington, DC

Utami, Z., A. Putra, Syafitri, and H. Dhia (2019). The Estimation of Geothermal Reservoir Temperature Using Geothermometer Equation in Cubadak Area, Pasaman Regency, West Sumatra, Indonesia. *Journal of Physics: Conference Series*, **1185**; 012018

Wioso, Y. B., Z. Wulandari, and D. Farhansyah (2022). Analyze Characteristic and Potential of Geothermal Energy in Danau Ranau, South Sumatera, Indonesia. In *Proceedings PIT IAGI 51st*. Makassar, Indonesia, pages 1–6

Zainal, P. A. A., E. Sutriyono, and M. M. Ibrahim (2024). Estimated Geothermal Reservoir Temperature Based on the Silica Geothermometer Method in the Ranau Lake Area and Surrounding Areas. *Journal of Science Research*, **26**(3); 376–380

